RSC Advances

PAPER

View Article Online
View Journal | View Issue

Cite this: *RSC Adv.*, 2017, **7**, 39383

One-pot extraction and aerobic oxidative desulfurization with highly dispersed V_2O_5/SBA-15 catalyst in ionic liquids†

Chao Wang,[a] Zhigang Chen,*[a] Xiaoyu Yao,[b] Wei Jiang,[c] Ming Zhang,[c] Hongping Li,[c] Hui Liu,[b] Wenshuai Zhu *[b] and Huaming Li[c]

Catalytic oxidation of thiophenic sulfides for separation from refined oils has turned out to be a hot topic from the angle of environmental protection. In this work, a series of pristine V_2O_5/SBA-15 composites, which could activate molecular oxygen (O_2) in air directly, have been prepared by a simple impregnation method. The successful loading and good dispersion of V_2O_5 on SBA-15 was, then, confirmed by multiple techniques. After this, one-pot extraction and aerobic oxidative desulfurization (EAODS) of oils was achieved under comparatively mild conditions. Here, sulfur removal of dibenzothiophene (DBT), as one of the most stubborn residuals in the hydro-desulfurization (HDS) process, could reach up to 99.3% (<3.5 ppm), meeting the latest restrict rules. In addition, excellent sulfur removal performance with different types of oils was achieved, indicating the practicability of this reaction system. A possible reaction process was proposed based on the results from electron spin-resonance spectroscopy (ESR), selective quenching experiments, and gas chromatography-mass spectrometry (GC-MS) measurement. Besides, the reaction system could be recycled at least 6 times without a significant decrease on sulfur removal.

Received 1st July 2017
Accepted 1st August 2017

DOI: 10.1039/c7ra07286d

rsc.li/rsc-advances

1. Introduction

Environmental issues, such as fog and haze, acid rain, and photochemical smog, have been threatening people's health in recent years, especially in developing countries. One of the main reasons is the combustion of traditional fossil fuels.[1] Sulfur compounds remaining in the refined oils could be burned to SO_x in vehicle engines.[2] Thus, many regulations have been introduced to decrease the sulfur content in fuels. In modern industry, hydro-desulfurization (HDS) has been widely used. In this process, sulfur compounds are converted to hydrogen sulfide (H_2S) in a hydrogen (H_2) atmosphere with the help of catalysts. However, its reaction temperature and pressure are very high (>630 K, >8 MPa) and sulfur removal for some aromatic sulfur compounds is still relatively low.[3] From the angle of sustainable development, deep desulfurization methods with high selectivity to thiophenic sulfides under comparatively mild reaction conditions are being sought.[4–7]

The aerobic oxidation method, as a novel oxidation method, has drawn much attention in the latest decades. Compared with many other oxidants, such as hydrogen peroxide (H_2O_2),[8–10] ozone (O_3),[11] *tert*-butylhydroperoxide (TBHP),[12] and nitrogen dioxide (NO_2),[13] molecular oxygen (O_2) existed in the air can be used as oxidant directly without any pre-treatments (purification or cryogenic separation) in this process. Thence, oxidative desulfurization (ODS) with O_2, known as aerobic ODS, is widely concerned these years.[14] However, the activation of O_2 is still challenging under compared mild conditions. In recent years, many catalysts, such as organic framework materials,[15] nano-materials,[16] noble metals,[17] porphyrin,[18] and polyoxomolybdates,[19] have been synthesized and employed in aerobic ODS process. Yet, these catalysts are hard to be applied in large scale production process, as their complicated synthesize process or their expensive cost.

Transition metal oxides (TMOs), as a group of common metal oxides, are widely used in many fields as their outstanding chemical properties.[20] In recent years, aerobic oxidative reactions with economic TMOs have been explored.[21] Shen *et al.*[22] found that aerobic oxidization of CO could be realized with using Co_3O_4 as catalyst under mild conditions. Tang *et al.*[23] developed a copper–manganese oxide catalyst ($Mn_{1.5}Cu_{1.5}O_4$) and tested its activity for aerobic oxidation of benzyl alcohol, achieving remarkable conversion under atmosphere pressure. Recently, Zhang *et al.*[24] proved that aerobic ODS could be realized with using Ce–Mo–O catalyst under compared mild conditions. However, aggregation phenomenon

[a]School of the Environment and Safety Engineering, Jiangsu University, 301 Xuefu Road, Zhenjiang 212013, P. R. China. E-mail: chenzg01@126.com
[b]School of Chemistry and Chemical Engineering, Jiangsu University, 301 Xuefu Road, Zhenjiang 212013, P. R. China. E-mail: zhuws@ujs.edu.cn
[c]Institute for Energy Research, Jiangsu University, 301 Xuefu Road, Zhenjiang 212013, P. R. China

† Electronic supplementary information (ESI) available. See DOI: 10.1039/c7ra07286d

is often observed in many bulk TMOs, which makes less active sites to be exposed.

Thus, many carriers (MCM-41,[25,26] SBA-15,[27] ZSM-5,[28] Al_2O_3 [29]), which might be used to disperse these active species have been developed. Among these carries, SBA-15 is often selected as its outstanding thermal stability, high specific surface area, uniform pore, and large pore volume.[30,31] In addition, extraction coupled with oxidative desulfurization (EODS) has also been concerned by many researchers.[32,33] Ionic liquids (ILs), as a group of fantastic solvents compared with traditional organic solvents, are often introduced in many EODS reaction systems.[34,35] Here, sulfur compounds are firstly extracted to IL phase, and oxidized to sulfones subsequently. As the immiscibility between oils and ILs, clean oils could be separated easily by a simple decantation method after reaction. However, to date, works about EODS with using O_2 as oxidant are still scarcely reported.

With these contributions, we have explored the possibility of using economic supported TMOs and ILs for extraction and aerobic oxidative desulfurization (EAODS) reaction under compared mild conditions. In this work, V_2O_5/SBA-15 composites were synthesized by a simple impregnation method. The well dispersion of V_2O_5 on SBA-15 made it possible to expose more active sites than bulk materials. Finally, a simple EAODS reaction system consisted of V_2O_5/SBA-15, air and IL has been developed. Here, sulfur removal of dibenzothiophene (DBT), as a refractory residual in HDS process, could reach up to 99.3% (<3.5 ppm), meeting the latest strict rules. In addition, oils with different S-concentrations, substrates, aromatics/olefins addition all show wonderful sulfur removal, making this reaction system possible to be applied in practical production process. Moreover, this reaction system could be recycled at least 6 times without a significant decrease on sulfur removal.

2. Experimental

2.1. Synthesis procedures of the catalysts

The details about reagents used in this work are listed in ESI†.

Pure siliceous SBA-15 is synthesized according to the procedures reported previously.[36] Here, poly(ethylene glycol)-*block*-poly(propylene glycol)-*block*-poly(ethylene glycol) P123 and tetraethyl orthosilicate (TEOS) are used as the template and silica source, respectively. Then, SBA-15 is dispersed in a beaker containing 50 mL H_2O and a certain amount of ammonium metavanadate (NH_4VO_3). The beaker is, then, set in oil bath (40 °C) with constant stirring for 20 h. After this, H_2O is evaporated out with a higher temperature environment (80 °C) in oil bath with constant stirring. At last, the obtained powder is calcined to 600 °C and retained for 300 min in muffle furnace at the rate of 2 °C min^{-1}. The as-prepared catalysts with different mass percentages of V loading amount are marked as 1 wt% V_2O_5/SBA-15, 2 wt% V_2O_5/SBA-15, 5 wt% V_2O_5/SBA-15 and 10 wt% V_2O_5/SBA-15, respectively. Here, 5 wt% V_2O_5/SBA-15 (as an example) means the mass percentage of V_2O_5 in the catalyst is 5%, and the mass percentage of SBA-15 in the catalyst is 95%.

The equipment used to characterize the as-prepared catalysts is listed in ESI.†

2.2. EAODS reaction process

The preparation procedures of different oils are listed in ESI.†

The EAODS reaction process is carried out in a 150 mL round-bottomed flask. Firstly, 0.05 g catalyst, 5 mL IL (1-butyl-3-methylimidazolium tetrafluoroborate, [Bmim]BF_4), and 50 mL oil are added together. Then, fresh air (100 mL min^{-1}) is introduced to the reaction system by an air pump. After this, the flask is set in oil bath (120 °C) to maintain a constant reaction temperature.

Gas chromatography with flame ionization detector (GC-FID) is used to evaluate the sulfur content in oils. The detailed procedures of GC are listed in ESI.† The reacted oil is collected every 30 min. The conversion of sulfur compounds in oils is used to indicate the removal of sulfur compounds, which is accepted by almost all researchers in the field of oxidative desulfurization. Sulfur removal is calculated as shown in eqn (1), where C_0 (ppm) is the initial sulfur concentration and C_t (ppm) is the transient sulfur concentration at any time t (min) in oils. After reaction, the oil phase and the IL phase are separated, collected and further analyzed by gas chromatography-mass spectrometer (GC-MS) measurement. The detailed procedures of GC-MS are listed in IS.

$$\text{Sulfur removal (\%)} = (1 - C_t/C_0) \times 100\% \quad (1)$$

3. Results and discussion

3.1. Characterization of the as-prepared catalysts

The morphologies and structures of the as-prepared catalysts are characterized by the following measurements. Firstly, scanning electron microscope (SEM) and transmission electron microscope (TEM) images of the catalysts were given to investigate the morphology changes of V_2O_5. As can be seen in Fig. 1(a) and (b), bulk V_2O_5 exhibits a rod-like shape (about 5 μm long) and aggregate together. In Fig. 1(c), many ropelike domains with relatively uniform size (about 1 μm) are found, which is agree with a typical SBA-15 morphology.[37] Meanwhile, well-ordered hexagonal arrays of mesoporous structures are clearly observed in Fig. 1(d), indicating a typical SBA-15 material. While for V_2O_5/SBA-15, its morphology is similar to pure SBA-15, and no rod-like shape structure could be seen, indicating the high dispersion of V_2O_5 on SBA-15 (Fig. 1(e)). However, many black particles are observed in TEM image (Fig. 1(e)), which could be attributed to the existence of V_2O_5 particles. These observed particles are much smaller than bulk V_2O_5. Then, the introduction of V element was further confirmed by EDS analysis (Fig. 1(g) and (h)). The observed well distribution of Si, O, and V elements in Fig. 1(g) also indicate that V_2O_5 is dispersed uniformly on SBA-15, which is different from bulk V_2O_5.

In order to confirm the value state of the elements existed on the surface of the catalyst, X-ray photoelectron spectroscopy (XPS) analysis of 5 wt% V_2O_5/SBA-15 was conducted and displayed in Fig. 2. The observed Si 2p peak at 103.4 eV and O 1s peak at 532.9 eV in Fig. 2(b) and (c) are corresponded to Si and O elements in SBA-15, respectively.[36,38] Besides, the oxidation state of V element was also studied after a Shirley background subtraction

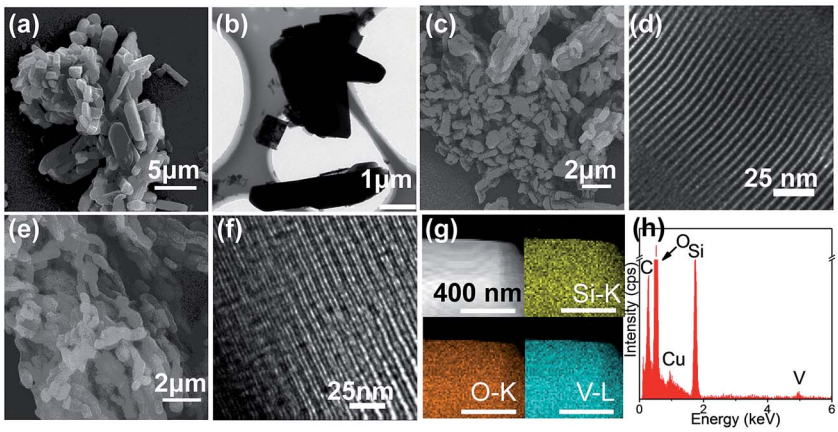

Fig. 1 SEM and TEM images of bulk V_2O_5 (a and b), pure SBA-15 (c and d), 5 wt% V_2O_5/SBA-15 (e and f), EDS analysis of 5 wt% V_2O_5/SBA-15 (g and h).

(Fig. 2(d)). Peaks at 517.2 eV and 524.5 eV are observed, which are corresponded to V(v) $2p_{3/2}$ and V(v) $2p_{1/2}$ in V_2O_5.[39] Besides, peaks at 516.3 eV and 523.6 eV are also observed, which are corresponded to V(IV) $2p_{3/2}$ and V(IV) $2p_{1/2}$.[39,40] The existence of V(IV) could be ascribed to the loss of lattice oxygen in V_2O_5 during the synthesize process under high temperature (600 °C) conditions, which is commonly seen in many TMOs including V_2O_5.[41,42] The existence of lattice oxygen vacancy might induce a higher aerobic catalytic performance.[43,44] Here, we might guess that the V elements dispersed on SBA-15 are mainly existed in the form of V_2O_5. Besides, the elements distribution of different elements from XPS analysis was given in Table S1.† After a series of calculation, the mass ratio of V_2O_5 on the surface of the catalysts is ~4.2 wt%, as some V_2O_5 might enter into the channels of SBA-15. This speculation would be verified in a further step by the following experiments, especially by BET analysis.

The crystal structure of the catalysts was verified in a further step by wide-angle X-ray diffraction (XRD) and Raman measurements, as two characterization methods which are sensitive to metal oxides especially. In Fig. 3(a), a broad diffraction peak of pure SBA-15 is observed at $2\theta \approx 23°$, which is corresponded to the characteristic peak of amorphous SiO_2. For bulk V_2O_5, the characteristic peaks observed can be assigned to its orthorhombic phase (JCPDS 85-0601). Though characteristic peaks of V_2O_5 become weaker in V_2O_5/SBA-15 composite, some of them can still be observed. The other characteristic peaks might be submerged in the peaks of SBA-15. Thus, Raman measurement, which is sensitive to V_2O_5 but have no response to SBA-15 was conducted subsequently (Fig. 3(b)). Though the

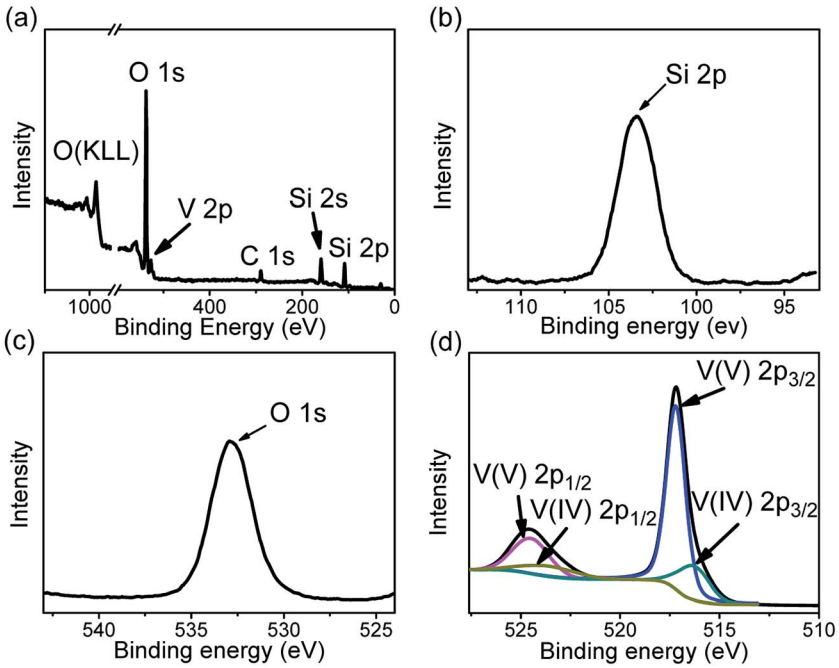

Fig. 2 XPS spectrum of 5 wt% V_2O_5/SBA-15 (a), high resolution spectra of Si 2p (b), O 1s (c), and V 2p (d).

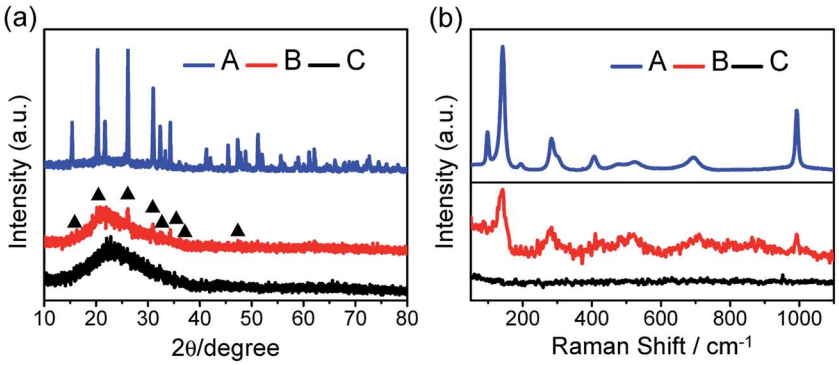

Fig. 3 Wide-angle XRD patterns (a) and Raman shifts (b) of the as-prepared catalysts. (A) bulk V_2O_5, (B) 5 wt% V_2O_5/SBA-15, (C) pure SBA-15. (▲) The observed characteristic peaks of V_2O_5 in V_2O_5/SAB-15 composite.

peaks intensity decreases sharply, almost all characteristic peaks of V_2O_5 could be found in V_2O_5/SBA-15 composite. The deceased characteristic peaks of metal oxide might be induced by its low loading amount and excellent dispersion. Combining the above results, we might preliminary conclude that V_2O_5 is loaded on SBA-15 successfully with high dispersion.

To verify whether the introduction of V_2O_5 would destroy the mesoporous structure of SBA-15, low-angle XRD and BET analysis of the as-prepared catalysts were collected and displayed in Fig. 4. Three peaks can be observed between $2\theta = 0$–4° from the low-angle XRD patterns. The strongest peak, around $2\theta = 0.8^\circ$, is corresponded to (100) diffraction. Another two weaker peaks, around $2\theta = 1.6, 1.8^\circ$, are corresponded to (110), (200) diffraction, respectively.[38] These peaks observed at low-angle range indicate that all of these synthesized materials exhibit a highly ordered 2D hexagonal mesoporous structure ($p6mm$).[45] Besides, the introduction of V_2O_5 would not destroy the mesoporous structure of SBA-15.

In Fig. 4(b), N_2 absorption–desorption isothermals of the as-prepared catalysts were collected to investigate their mesoporous structure in a further step. Pure SBA-15 exhibit a typical IV isotherm curve with H1-type hysteresis loop according to IUPAC classification,[46] which is a typical mesoporous structure. The sharp inflection between $P/P_0 = 0.5$ and $P/P_0 = 0.8$ is observed, which is caused by the desorption of nitrogen and capillary condensation in the pore structure. Similarly, IV isotherm is maintained after the introduction of V_2O_5, indicating that the cylindrical channels mesoporous structure is remained. In addition, BJH pore size distribution curves of the as-prepared samples are also given (Fig. 4(b) inset). Pore diameter of the as-prepared catalyst decreases from 8 nm to 5 nm as the loading amount of V_2O_5 on SBA-15 increases from 0 to 10 wt%, indicating that parts of V_2O_5 might enter into mesoporous channels in SBA-15. At last, the structure and texture parameters of all these five samples were summarized and listed in Table 1. Combining the above all results, we can reasonably speculate that the dispersion of V_2O_5 on SBA-15 would reduce the agglomeration of metal oxide, and would not destroy the mesoporous structure of the carrier simultaneously.

Table 1 The structure properties of the as-prepared catalysts

Samples	S_{BET} ($m^2\ g^{-1}$)	Pore volume ($cm^3\ g^{-1}$)	Pore size (nm)
SBA-15	774	1.02	5.7
1 wt% V_2O_5/SBA-15	622	0.92	5.4
2 wt% V_2O_5/SBA-15	586	0.68	5.2
5 wt% V_2O_5/SBA-15	547	0.61	5.1
10 wt% V_2O_5/SBA-15	481	0.55	5.0

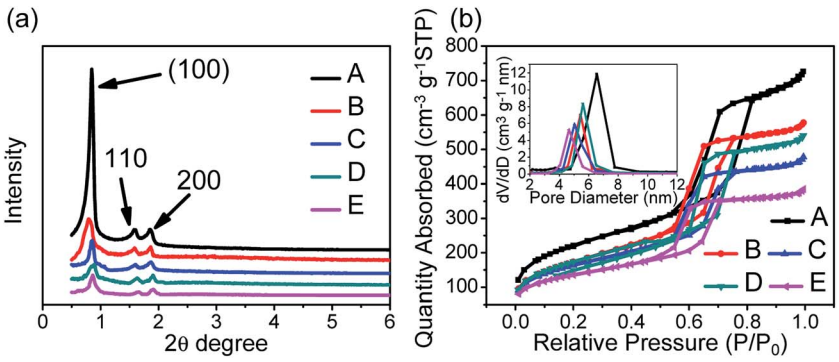

Fig. 4 Low-angle XRD patterns (a) and BET analysis (b) of the as-prepared catalysts. (A) Pure SBA-15, (B) 1 wt% V_2O_5/SBA-15, (C) 2 wt% V_2O_5/SBA-15, (D) 5 wt% V_2O_5/SBA-15, (E) 10 wt% V_2O_5/SBA-15.

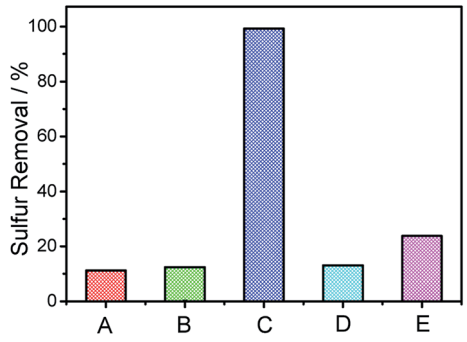

Fig. 5 Sulfur removal with different reaction systems. (A) IL, (B) IL + air, (C) IL + air + catalyst, (D) IL + N_2 + catalyst, (E) air + catalyst. Experimental conditions: $T = 120$ °C, V(oil) = 50 mL, V([Bmim]BF_4) = 5 mL, m(catalyst) = 0.05 g, $t = 4$ h, v(air) = 100 mL min^{-1}.

3.2. Sulfur removal with different reaction systems

Sulfur removal with different reaction systems were conducted and shown in Fig. 5. Sulfur removal observed with only IL could be attributed the extraction ability of IL. When fresh air is introduced, sulfur removal is almost the same with only extraction, which demonstrate that O_2 in air could not be activated by IL. But, when 5 wt% V_2O_5/SBA-15 is added, sulfur removal of DBTincreases sharply to 99.3% (<3.5 ppm), indicating the catalytic ability of the as-prepared catalyst. Besides, blank experiments were also conducted to clarify the roles of O_2 and IL in EAODS process. Firstly, air introduced into the reaction system is replaced by high pure nitrogen (N_2). As a result, sulfur removal decreases sharply after reaction for 4 h, which suggests that active oxygen species are generated from O_2 in air. Then, another blank experiment was conducted without IL addition. As a result, sulfur removal also decreases sharply after reaction for 4 h, which illustrates that EAODS system could accelerate the reaction rate obviously. Now, we might conclude that the as-prepared catalyst, the air introduced and the IL added all play important roles in desulfurization process.

3.3. Optimization of oxidative desulfurization parameters

Sulfur removal of oils with different catalysts were studied and listed in Table 2. When the loading amount of V_2O_5 increases, sulfur removal increases accordingly. However, when the loading amount increases to 10 wt%, sulfur removal increases slightly. Thus, 5 wt% V_2O_5/SBA-15 is selected in the following experiments. Besides, sulfur removal with SBA-15, bulk V_2O_5 and simple mix of V_2O_5 and SBA-15 were also investigated, respectively. When SBA-15 is selected, no aerobic ODS activity could be observed. When bulk V_2O_5 and simple mix of V_2O_5 and SBA-15 are selected, sulfur removal could be realized, but less than the sulfur removal obtained with V_2O_5/SBA-15. All these data indicate that the high dispersion of V_2O_5 on SBA-15 could help to expose more active sites, which could induce a higher a sulfur removal directly.

Table 2 Sulfur removal of oils with different catalysts[a]

Entry	Catalyst	Sulfur removal/%
1	SBA-15	12.2
2	1 wt% V_2O_5/SBA-15	76.4
3	2 wt% V_2O_5/SBA-15	96.1
4	5 wt% V_2O_5/SBA-15	99.3
5	10 wt% V_2O_5/SBA-15	99.4
6	Bulk V_2O_5	43.2
7	SBA-15 + V_2O_5	44.5

[a] Experiment conditions: $T = 120$ °C, V(oil) = 50 mL, V([Bmim]BF_4) = 5 mL, m(catalyst) = 0.05 g, $t = 4$ h, v(air) = 100 mL min^{-1}.

In addition, sulfur removal with different ILs were investigated and displayed in Table S2.† Here, deep desulfurization could be achieved when [Bmim]BF_4 is selected. However, sulfur removal decreases when other ILs are selected. From the obtained data, we could find that ILs with shorter carbon chain imidazolium cation could induce higher sulfur removal, when they share the same anion. And ILs with BF_4^- as anion would obtain higher sulfur removal, when they share the same cation. The above regularities are consisted with the previous reported EODS reaction systems.[47,48] In addition, sulfur removal without any IL deceases sharply, indicating the indispensable role plays by IL. Finally, [Bmim]BF_4 is selected in the following studies.

3.4. Sulfur removal of oils with different S-concentrations and substrates

Considering the fact that the concentrations, and categories of sulfur compounds are different from each other in refined oils, sulfur removal with oils of different S-concentrations, substrates were conducted (Fig. 6). For Fig. 6(a), in the beginning 1.5 h, sulfur removal of 4 different oils tested here is still very low, which is a common phenomenon appeared in many other aerobic ODS reaction systems.[15,49,50] After reaction for 4 h, deep desulfurization could be realized with the oil of 500 ppm S-concentration. When the S-concentration in oils increases from 600 to 1000 ppm, sulfur removal for these oils could reach up to 99.7%, 97.6% and 95.3% after reaction for 7 h, respectively. All the obtained data show the excellent sulfur removal ability of this aerobic ODS system, which is superior to many other ODS systems with using H_2O_2 as oxidant.

In Fig. 6(b), sulfur removal with 4-methyl dibenzothiophene (4-MDBT) and 4,6-dimethyl dibenzothiophene (4,6-DMDBT) were also studied under the same reaction conditions. Sulfur removal at $t = 0$ h decreases as: DBT > 4-MDBT > 4,6-DMDBT, which illustrates the extractive desulfurization (EDS) ability of IL. This might be influenced by the electron affinity, electrophilicity of these three different sulfur compounds according to the previous study.[51] After reaction for 6 h, sulfur removal of all these three different sulfur compounds could reach up to >95%, indicating the excellent sulfur removal ability of this reaction system. Besides, the final sulfur removal also decreases as: DBT > 4-MDBT > 4,6-DMDBT. This could be explained by the differences of Fukui functions of S atom in sulfides and the steric hindrance effect of methyl according to the previous studies.[51,52]

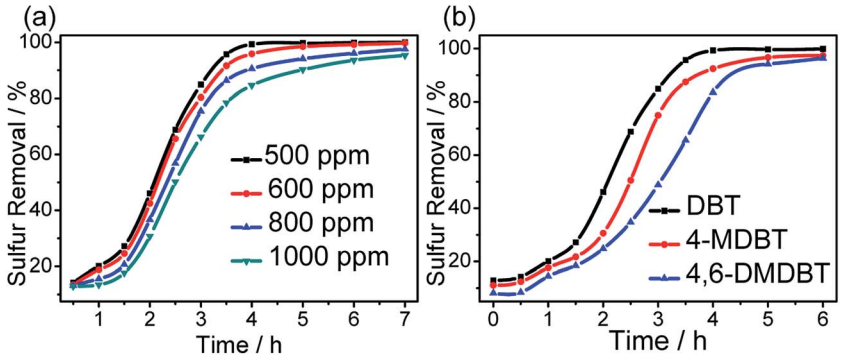

Fig. 6 Sulfur removal of oils with different S-concentrations (a), and substrates (b). Experimental conditions: $T = 120$ °C, V(oil) = 50 mL, V([Bmim]BF_4) = 5 mL, m(catalyst) = 0.05 g, v(air) = 100 mL min^{-1}.

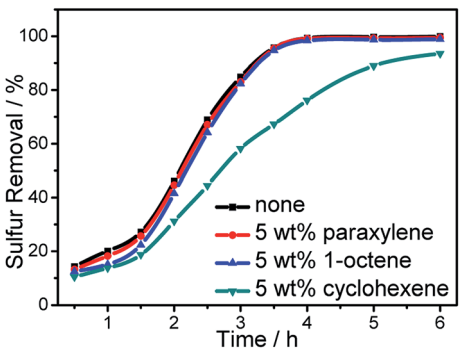

Fig. 7 Effect of the co-existence of olefins and aromatics on sulfur removal. Experimental conditions: T = 120 °C, V(oil) = 50 mL, V([Bmim]BF_4) = 5 mL, m(catalyst) = 0.05 g, v(air) = 100 mL min^{-1}.

3.5. Effect of the co-existence of olefins and aromatics on sulfur removal

In Fig. 7, the influence of the co-existence of aromatics and olefins, as two common hydrocarbons existed in refined oils, was also studied. Here, sulfur removal with oils of 5 wt% paraxylene and 5 wt% 1-octene additions could still reach up to 99.1% and 98.6%, respectively. However, when cyclohexene is selected, sulfur removal decreases sharply from 2 h to 5 h. As ring-opening reaction of cyclohexene is carried out easily, the oxidization of sulfur compounds and cyclohexene is carried out simultaneously, leading a significant slower kinetics for desulfurization reaction. Though the removal of sulfide is disturbed, sulfur removal could still reach up to 93.5%, which is superior to many previous studies.[53]

Considering the powerful sulfur removal of this reaction system, sulfur removal of real diesel oil (from PetroChina Co Ltd. without any desulfurization treatment) was conducted (Fig. S1†). Here, the initial S-concentration of diesel oil is ~950 ppm. As the complex composition of sulfides and the co-existence of the olefins and aromatics in actual diesel oil, double amount of the catalyst and ionic liquid is used here. Though sulfur removal could reach up to >95% after reaction for 12 h, ~47 ppm sulfides is still existed in the diesel oil phase. From the above all experiments, we speculate that this EAODS might be more suitable for oils after a preliminary HDS process, as the initial S-concentration and the content of olefins would decreased sharply after the preliminary HDS process.

3.6. Recycling performance of this reaction system

Recycling performance of a reaction system, as a very important index in industrial manufacture process, was investigated (Fig. 8). After reaction, the upper oil phase is separated out by a simple decantation method. Then, fresh oil is added into the reaction flask. Sulfur removal could still reach up to >90% after recycling for 6 times, indicating a wonderful recycling performance. Besides, the EDS performance of IL decreases simultaneously, which might be caused by the saturation of sulfones in IL phase as needle-like crystals is observed in flask wall (Fig. 8 inset). The saturation of sulfones in IL phase might be the critical factor which would influences the final EAODS performance directly. The remarkable recycling performance of this reaction system made it possible to be applied in industrial application.

3.7. Possible reaction process of this reaction system

In order to confirm the active species generated in EAODS system, X-band electron spin-resonance spectroscopy (ESR) signals of different reaction systems were investigated (Fig. 9(a)). Here, 5,5-dimethyl-1-pyrroline N-oxide (DMPO) is used as a spin trap. Characteristic peaks of typical DMPO-$O_2^{-\bullet}$ are observed in the

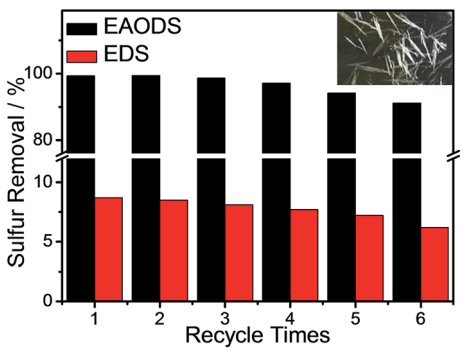

Fig. 8 Investigation of the recycling performance of reaction system. Experimental conditions: $T = 120$ °C, V(oil) = 50 mL, V([Bmim]BF_4) = 5 mL, m(catalyst) = 0.05 g, t = 4 h, v(air) = 100 mL min^{-1}.

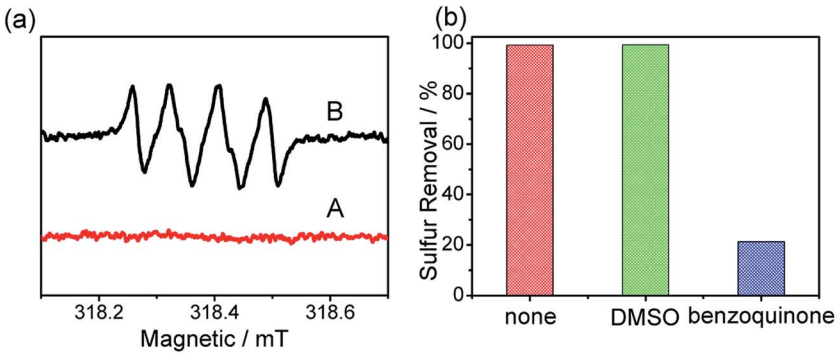

Fig. 9 ESR spectra of DMPO-$O_2^{-\bullet}$ adduct in different reaction system (a), investigation of selective quenching experiments (b). (A) With catalyst addition, (B) without catalyst addition, n(DMOS) = n(benzoquinone) = n(DBT).

reaction system with catalyst addition.[54] The detected radical might be generated from the reaction between O_2 in the air and the added catalyst. The generation of $O_2^{-\bullet}$ in EAODS process was further verified by selective quenching experiments (Fig. 9(b)). Here, benzoquinone and dimethyl sulphoxide (DMSO) are selected as quenchers of $O_2^{-\bullet}$ and HO$^\bullet$, respectively.[24] When DMSO is added into the reaction system, no variety of final sulfur removal is observed. Whereas, when benzoquinone is added, the finally sulfur removal decreases sharply, indicating the production of $O_2^{-\bullet}$ in this reaction process.

Based on the above results, the reaction process of this EAODS system was proposed as follows (Scheme 1). Sulfide is first extracted into the IL phase to form a partial high S-concentration. Meanwhile, V(IV) existed in the catalyst could transfer an electron (e^-) to the O_2 absorbed on SBA-15 to achieve $O_2^{-\bullet}$. As a strong oxidant, $O_2^{-\bullet}$ could oxidize sulfides to their corresponding sulfones, and release an extra electron (e^-). Then, the released electron (e^-) could be captured by other O_2 to form $O_2^{-\bullet}$, or be captured by other V(V) to form V(IV) again. Thus, endless active oxide species could be generated in this recycling process.

Then, GC-MS analysis of oxidized products was conducted to further confirm the proposed process (Fig. S2†). In oil phase, no other sulfur species could be detected after reaction except the tiny residuals, indicating that sulfides were separated from oils phase effectively. Whereas, sulfur compounds and their corresponding sulfones could be observed in IL phase simultaneously, indicating that sulfur compounds are first extracted to the IL phase and then selectively oxidized to their corresponding sulfones. The above results illustrate that deep removal of sulfides could be achieved with this EAODS procedure, and the proposed reaction process is confined simultaneously.

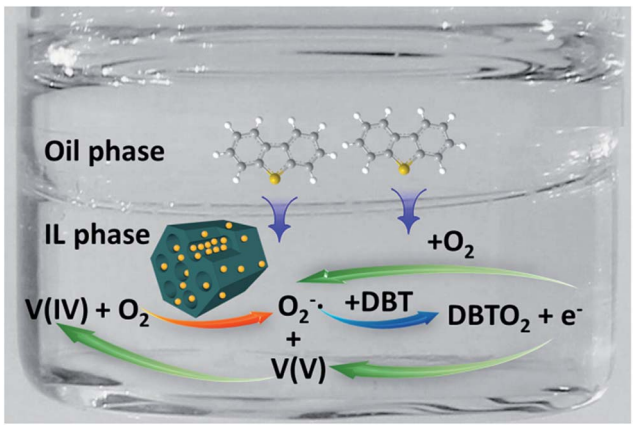

Scheme 1 The proposed reaction process.

4. Conclusions

In summary, highly dispersed V_2O_5/SBA-15 composites were synthesized through a simple impregnation method. The morphologies and structures of the composites were confirmed by a series of characterization methods. Then, a simple liquid–liquid EAODS reaction system composed of O_2, V_2O_5/SBA-15, and IL for deep removal (99.3%, <3.5 ppm) of sulfur compounds in oils has been developed under compared mild conditions. Sulfur compounds in oils are firstly extracted into IL phase and oxidized to their corresponding sulfones by the produced $O_2^{-\bullet}$ subsequently. Oils with different S-concentrations, substrates, olefins/aromatics additions all show wonderful sulfur removal. Finally, a possible reaction process is proposed according to the results of ESR, selective quenching experiments, and GC-MS measurement. The superiorities of this reaction system, such as low cost of the catalysts, compared mild reaction conditions, deep desulfurization for different oils, and excellent recycling performance, make this reaction system potentially promising for practical applications.

Acknowledgements

This work was financially supported by the National Nature Science Foundation of China (Nos. 21376111, 21576122, 21506080), Natural Science Foundation of Jiangsu Province (No. BK20150485), Postdoctoral Foundation of China (No. 2015M570412), Graduate Education Innovation Project of Jiangsu Province (KYLX16_0911).

References

1 X. L. Wang, Z. Zhao, P. Zheng, Z. T. Chen, A. J. Duan, C. M. Xu, J. Q. Jiao, H. L. Zhang, Z. K. Cao and B. H. Ge, *J. Catal.*, 2016, **344**, 680–691.

2 Y. R. Wang, M. Liu, A. F. Zhang, Y. Zuo, F. S. Ding, Y. Chang, C. S. Song and X. W. Guo, *Ind. Eng. Chem. Res.*, 2017, **56**, 4709–4717.
3 C. P. Li, J. J. Zhang, Z. Li, J. M. Yin, Y. N. Cui, Y. Liu and G. Yang, *Green Chem.*, 2016, **18**, 3789–3795.
4 Q. Lü, G. Li and H. Y. Sun, *Fuel*, 2014, **130**, 70–75.
5 A. Ishihara, D. H. Wang, F. Dumeignil, H. Amano, E. W. H. Qian and T. Kabe, *Appl. Catal., A*, 2005, **279**, 279–287.
6 X. J. Wang, W. Y. Yang, F. T. Li, Y. B. Xue, R. H. Liu and Y. J. Hao, *Ind. Eng. Chem. Res.*, 2013, **52**, 17140–17150.
7 Y. S. Shen, X. H. Xu and P. W. Li, *RSC Adv.*, 2012, **2**, 6155–6160.
8 J. Zhang, A. J. Wang, Y. J. Wang, H. Y. Wang and J. Z. Gui, *Chem. Eng. J.*, 2014, **245**, 65–70.
9 L. T. Li, J. S. Zhang, C. Shen, Y. J. Wang and G. S. Luo, *Fuel*, 2016, **167**, 9–16.
10 Y. Chen and Y. F. Song, *Ind. Eng. Chem. Res.*, 2013, **52**, 4436–4442.
11 C. H. Ma, D. Chen, F. P. Liu, X. S. Sun, F. R. Xiao and B. Dai, *RSC Adv.*, 2015, **5**, 96945–96952.
12 A. Bazyari, A. A. Khodadadi, A. H. Mamaghani, J. Beheshtian, L. T. Thompson and Y. Mortazavi, *Appl. Catal., B*, 2016, **180**, 65–77.
13 V. C. Srivastava, *RSC Adv.*, 2012, **2**, 759–783.
14 W. Zhang, H. Zhang, J. Xiao, Z. X. Zhao, M. X. Yu and Z. Li, *Green Chem.*, 2014, **16**, 211–220.
15 A. Gomez-Paricio, A. Santiago-Portillo, S. Navalon, P. Concepcion, M. Alvaro and H. Garcia, *Green Chem.*, 2016, **18**, 508–515.
16 C. Yu, L. M. Fan, J. Yang, Y. Y. Shan and J. S. Qiu, *Chem.–Eur. J.*, 2013, **19**, 16192–16195.
17 F. Lin, Y. N. Zhang, L. Wang, Y. L. Zhang, D. E. Wang, M. Yang, J. H. Yang, B. Y. Zhang, Z. X. Jiang and C. Li, *Appl. Catal., B*, 2012, **127**, 363–370.
18 X. R. Zhou, S. Lü, H. Wang, X. N. Wang and J. H. Liu, *Appl. Catal., A*, 2011, **396**, 101–106.
19 N. F. Tang, Z. X. Jiang and C. Li, *Green Chem.*, 2015, **17**, 817–820.
20 Y. Wang, J. Guo, T. F. Wang, J. F. Shao, D. Wang and Y. W. Yang, *Nanomaterials*, 2015, **5**, 1667–1689.
21 P. F. Zhang, H. F. Lu, Y. Zhou, L. Zhang, Z. Wu, S. Z. Yang, H. L. Shi, Q. L. Zhu, Y. F. Chen and S. Dai, *Nat. Commun.*, 2015, **6**, 8446.
22 X. W. Xie, Y. Li, Z. Q. Liu, M. Haruta and W. J. Shen, *Nature*, 2009, **458**, 746–749.
23 Q. H. Tang, X. N. Gong, P. Z. Zhao, Y. T. Chen and Y. H. Yang, *Appl. Catal., A*, 2010, **389**, 101–107.
24 Y. W. Shi, G. Liu, B. F. Zhang and X. W. Zhang, *Green Chem.*, 2016, **18**, 5273–5279.
25 X. Li, F. Zhou, A. J. Wang, L. Y. Wang and Y. K. Hu, *Ind. Eng. Chem. Res.*, 2009, **48**, 2870–2877.
26 T. Prasomsri, W. Jiao, S. Z. Weng and J. Garcia Martinez, *Chem. Commun.*, 2015, **51**, 8900–8911.
27 C. Lavenn, A. Demessence and A. Tuel, *J. Catal.*, 2015, **322**, 130–138.
28 M. L. Tsai, R. G. Hadt, P. Vanelderen, B. F. Sels, R. A. Schoonheydt and E. I. Solomon, *J. Am. Chem. Soc.*, 2014, **136**, 3522–3529.
29 P. A. Nikulshin, D. I. Ishutenko, A. A. Mozhaev, K. I. Maslakov and A. A. Pimerzin, *J. Catal.*, 2014, **312**, 152–169.
30 T. Wang, X. Yuan, S. R. Li, L. Zeng and J. L. Gong, *Nanoscale*, 2015, **7**, 7593–7602.
31 H. B. Xu, S. H. Zhou, L. L. Xiao, S. Z. Li, T. Song, Y. Wang and Q. H. Yuan, *Carbon*, 2015, **87**, 215–225.
32 H. Y. Song, J. J. Gao, X. Y. Chen, J. He and C. X. Li, *Appl. Catal., A*, 2013, **456**, 67–74.
33 H. Y. Lü, P. C. Li, C. L. Deng, W. Z. Ren, S. N. Wang, P. Liu and H. Zhang, *Chem. Commun.*, 2015, **51**, 10703–10706.
34 S. J. Zeng, H. S. Gao, X. C. Zhang, H. F. Dong, X. P. Zhang and S. J. Zhang, *Chem. Eng. J.*, 2014, **251**, 248–256.
35 H. S. Gao, S. J. Zeng, X. M. Liu, Y. Nie, X. P. Zhang and S. J. Zhang, *RSC Adv.*, 2015, **5**, 30234–30238.
36 W. J. Ding, W. S. Zhu, J. Xiong, L. Yang, A. M. Wei, M. Zhang and H. M. Li, *Chem. Eng. J.*, 2015, **266**, 213–221.
37 A. Shahbazi, H. Younesi and A. Badiei, *Chem. Eng. J.*, 2011, **168**, 505–518.
38 J. Xiong, W. S. Zhu, W. J. Ding, L. Yang, M. Zhang, W. Jiang, Z. Zhao and H. M. Li, *RSC Adv.*, 2015, **5**, 16847–16855.
39 W. Zhao, Q. Zhong, Y. X. Pan and R. Zhang, *Chem. Eng. J.*, 2013, **228**, 815–823.
40 V. V. Kaichev, G. Y. Popova, Y. A. Chesalov, A. A. Saraev, D. Y. Zemlyanov, S. A. Beloshapkin, A. Knop-Gericke, R. Schloegl, T. V. Andrushkevich and V. I. Bukhtiyarov, *J. Catal.*, 2014, **311**, 59–70.
41 B. C. Enger, R. Lodeng and A. Holmen, *Appl. Catal., A*, 2008, **346**, 1–27.
42 J. J. Liu, S. R. Zhang, Y. Zhou, V. Fung, L. Nguyen, D. E. Jiang, W. J. Shen, J. Fan and F. F. Tao, *ACS Catal.*, 2016, **6**, 4218–4228.
43 M. F. Luo, J. M. Ma, J. Q. Lu, Y. P. Song and Y. J. Wang, *J. Catal.*, 2007, **246**, 52–59.
44 V. P. Santos, M. F. R. Pereira, J. J. M. Orfao and J. L. Figueiredo, *Appl. Catal., B*, 2010, **99**, 353–363.
45 L. Peng, A. Philippaerts, X. X. Ke, J. Van Noyen, F. De Clippel, G. Van Tendeloo, P. A. Jacobs and B. F. Sels, *Catal. Today*, 2010, **150**, 140–146.
46 M. Bhagiyalakshmi, J. Y. Lee and H. T. Jang, *Int. J. Greenhouse Gas Control*, 2010, **4**, 51–56.
47 W. Jiang, W. S. Zhu, Y. H. Chang, Y. H. Chao, S. Yin, H. Liu, F. X. Zhu and H. M. Li, *Chem. Eng. J.*, 2014, **250**, 48–54.
48 W. Jiang, W. S. Zhu, H. M. Li, J. Xiong, S. H. Xun, Z. Zhao and Q. Wang, *RSC Adv.*, 2013, **3**, 2355–2361.
49 H. Y. Lü, W. Z. Ren, W. P. Liao, W. Chen, Y. Li and Z. H. Suo, *Appl. Catal., B*, 2013, **138**, 79–83.
50 M. Shi, D. Zhang, X. Yu, Y. M. Li, X. H. Wang and W. Yang, *Fuel Process. Technol.*, 2017, **160**, 136–142.
51 H. P. Li, W. S. Zhu, S. W. Zhu, J. X. Xia, Y. H. Chang, W. Jiang, M. Zhang, Y. W. Zhou and H. M. Li, *AIChE J.*, 2016, **62**, 2087–2100.
52 S. Otsuki, T. Nonaka, N. Takashima, W. H. Qian, A. Ishihara, T. Imai and T. Kabe, *Energy Fuels*, 2000, **14**, 1232–1239.
53 C. Wang, Z. G. Chen, W. Q. Zhu, P. W. Wu, W. Jiang, M. Zhang, H. P. Li, W. S. Zhu and H. M. Li, *Energy Fuels*, 2017, **31**, 1376–1382.
54 W. Jiang, W. S. Zhu, Y. H. Chang, H. M. Li, Y. H. Chao, J. Xiong, H. Liu and S. Yin, *Energy Fuels*, 2014, **28**, 2754–2760.

